Plasmonics (2012) 7:99–106
DOI 10.1007/s11468-011-9281-9

Optimization of the Field Enhancement and Spectral Bandwidth of Single and Coupled Bimetal Core–Shell Nanoparticles for Few-Cycle Laser Applications

Ying-Ying Yang · Edit Csapó · Yong-Liang Zhang · Frederik Süßmann · Sarah L. Stebbings · Xuan-Ming Duan · Zhen-Sheng Zhao · Imre Dékány · Matthias F. Kling

Received: 9 April 2011 / Accepted: 17 August 2011 / Published online: 3 September 2011

Abstract We have theoretically studied and optimized the field enhancement and temporal response of single and coupled bimetal Ag/Au core–shell nanoparticles (NPs) with a diameter of 160 nm and compared the results to pure Ag and Au NPs. Very high-field enhancements with an amplitude reaching 100 (with respect to the laser field centered at 800 nm) are found at the center of a 2-nm gap between Ag/Au core–shell dimers. We have explored the excitation of the bimetal core–shell particles by Fourier transform-limited few-cycle optical pulses and identified conditions for an ultrafast plasmonic decay on the order of the excitation pulse duration. The high-field enhancement and ultrafast decay makes bimetal core–shell particles interesting candidates for applications such as the generation of ultrashort extreme ultraviolet radiation pulses via nanoplasmonic field enhancement. Moreover, in first experimental studies, we synthesized small bimetal Ag/Au core–shell NPs and compared their optical response with pure Au and Ag NPs and numerical results.

Keywords Plasmonic absorption spectra · Nanoplasmonic field enhancement · Few-cycle laser pulses · Nanoparticle synthesis · Core–shell nanoparticles

Y.-Y. Yang · F. Süßmann · S. L. Stebbings · M. F. Kling (✉)
Max-Planck-Institut für Quantenoptik,
Hans-Kopfermann-Str. 1,
85748 Garching, Germany
e-mail: matthias.kling@mpq.mpg.de

Y.-Y. Yang · Y.-L. Zhang · X.-M. Duan · Z.-S. Zhao
Technical Institute of Physics and Chemistry,
Chinese Academy of Sciences,
100190 Beijing, China

Y.-Y. Yang
Institute of Semiconductor, Chinese Academy of Sciences,
100083 Beijing, China

E. Csapó · I. Dékány
Supramolecular and Nanostructured Materials Research Group of the Hungarian Academy of Sciences, University of Szeged,
Aradi Vt.1,
6720 Szeged, Hungary

M. F. Kling
King Abdullah Institute for Nanotechnology,
King Saud University,
Riyadh 11451, Saudi Arabia

Introduction

Within the past 20 years, intense ultrashort laser pulses have promoted new X-ray sources, laser-driven particle accelerators, and enabled the generation of attosecond pulses of extreme ultraviolet radiation (XUV) [1]. These novel light sources have a profound impact on fundamental research and the potential for observing and controlling the electronic motion in complex systems, where the response is not only dominated by a single electron but rather the coherent and collective motion of many electrons [2]. In nanostructured materials, the properties of the collectively oscillating electrons (plasmons) can be tuned via the size, shape, and material of the nanosized matter [3]. When few-cycle laser pulses illuminate, a (semi-) metallic nanostructure, ultrafast nanoplasmonic field dynamics can be initiated [4, 5]. The dephasing time of a nanolocalized plasmon is typically 1–100 fs, allowing coherent control of nanoscale energy localization with femtosecond laser light [6]. Collective electronic or fermionic motion in nanoplasmonic systems unfolds on much shorter attosecond timescales [4]. Understanding and controlling collective excitations in nano-

systems on attosecond and femtosecond timescales may enable the development of new (attosecond) XUV and X-ray light sources based on nanoplasmonic field enhancement [7] and ultimately lightwave electronics, operating at orders of magnitude higher speed than conventional electronics [8].

A recent example, where nanoplasmonic field enhancement of metallic nanoparticles has been exploited, is the generation of XUV light via high-harmonic generation (HHG) [7]. For time-resolved spectroscopy applications which utilize XUV light generated via this scheme, it is desirable to keep the plasmonic response as short as possible in order to facilitate the production of ultrashort XUV light pulses. At the same time, an intensity enhancement >100 with respect to the intensity of the incident laser pulse is needed in order to avoid the damage of the nanosystem by the laser (which occurs at intensities beyond 10^{11} W/cm^2 [9]), while still facilitating local intensities sufficient for HHG.

Au and Ag nanoparticles (NPs) produced by colloidal chemical methods [10–12] and lithographic techniques [13–15] have been intensively studied. They exhibit surface plasmon resonances in the visible and near-infrared (NIR) spectral ranges, which give rise to large-field enhancements [16, 17]. They are employed in widespread applications in, e.g., scanning optical microscopy [18, 19], optical communication [20], high-density computing and information storage on the nanoscale [21], as well as for biosensors [22]. Although resonantly excited Ag NPs can show larger field enhancements than Au NPs [12], they suffer from oxidation in ambient environments. It is thus desirable to protect Ag NPs with a thin layer of another inert material. The plasmonic resonance of Au is red-shifted with respect to Ag [12], such that a combination of the two materials has two particular advantages: (1) a thin Au layer can protect Ag NPs against oxidation and (2) the combination of Ag and Au might allow for an ultra-broadband plasmonic resonance spectrum supporting a unique combination of an ultrafast temporal response with sufficient field enhancement for, e.g., HHG.

Here, we have theoretically studied and optimized the optical properties and enhancement of bimetallic nanoantennas consisting of Ag/Au core–shell nanospheres and compared them to pure Ag and Au nanospheres. Bimetallic NPs were recently synthesized successfully by colloidal chemistry [10, 11]. Their synthesis and experimental characterization is well documented [12]; however, the numerical analysis and theoretical optimization of their optical properties with respect to reaching ideal conditions for an ultrafast response are limited [23]. In our numerical calculations, we find that bimetal nanoantennas exhibit high plasmonic field enhancement for a suitable aspect ratio of the core–shell system. Their plasmonic spectrum ranges from the visible to the NIR and facilitates an ultrafast temporal response. We furthermore computed the plasmonic properties of strongly coupled bimetal nanoparticle dimers, which may be prepared by self-assembly methods [24]. The coupling between the nanoparticles of such assemblies allows for higher field enhancement as compared to single bimetal nanoparticles.

We also synthesized small bimetal core–shell particles and compared their plasmonic absorption spectra to our theoretical calculations. The bimetal core–shell nanoparticles shown here could only be fabricated as spheres with an overall radius in the range of a few nanometers using the present synthesis technique [25–27]. These particles tend to take polygonal shapes with larger dimensions [28]. Even these small bimetal nanoparticles, however, show the principal trends that we have observed in the calculations for single bimetal core–shell NPs.

Our theoretical and experimental work is motivated by the potential ultrafast plasmonics applications of bimetal NPs. A strong local field with sufficient amplitude caused by nanoplasmonic field enhancement can drive strong-field processes similar to a much stronger few-cycle laser field. The desire to keep the plasmonic response ultrashort are analogues to the change from a long laser pulse to a few-cycle laser pulse [4, 29, 30]: (1) tunneling ionization can be restricted to one dominant half cycle of the field, (2) recollision, driven by the local field, can be restricted to a single event, and (3) high-harmonic generation can be restricted such that the generation of single attosecond pulses is feasible [31].

Numerical Methods

In our calculations, we employed the finite difference time domain method (Lumerical, version 7.5) [32] to calculate the optical response of the metal and bimetal nanoparticles. The real and imaginary parts of the wavelength-dependent dielectric functions for Au and Ag were determined using the modified Debye model [33]. In our theoretical modeling, the nanoparticles are surrounded by vacuum (index of refraction, $n=1$). We calculated a total volume of a $1\times1\times1$ μm^3 and used a perfect matched layer boundary with a thickness of 500 nm to terminate the volume [34]. The three-dimensional mesh in the calculations has a unit size of $0.5\times0.5\times0.5$ nm^3 to ensure an accurate description of the near-field of the antennas [35]. For the NP dimers, the polarization direction of the excitation field was chosen to be along the longitudinal axis, along which the NPs are assembled.

The goals in our optimizations of the bimetal core–shell nanoparticles were twofold: (1) to optimize the resonance frequency of the particles to facilitate the highest possible field enhancement in combination with a few-cycle 800 nm Ti:sapphire excitation source and (2) to optimize the nanoplasmonic field enhancement to allow for HHG using such structures while avoiding their damage by the laser [9]. For the latter, considering a damage threshold of ca.

10^{11} W/cm^2, an enhancement in the field of above ca. 25 is required to generate XUV light in Xe gas injected into the region of large-field enhancement [31]. Our calculations indicate that such high-field enhancement cannot be achieved with single metal or bimetal spherical nanoparticles but may be achieved with coupled nanoparticles.

Optimization of the Optical Properties of Single Au/Ag Core–Shell Nanoparticles

The Ag/Au bimetal particles that have been studied here consist of an Ag core and an Au shell and are depicted in Fig. 1a. Both the resonance frequency and the local field enhancement can be tuned by adjusting the composition and size of the bimetallic nanoparticles. Therefore, we first carried out simulations with variable thicknesses d_{Au} of the Au shell ranging from d_{Au}=0 nm (pure Ag particles) to d_{Au}=80 nm (pure Au particles). This range is accessible by current synthesis techniques [36]. The overall radius of the sphere was fixed at R=80 nm. In order to compute the plasmonic absorption spectrum, the nanoparticles are illuminated with a continuous plane wave with normalized electric field amplitude for each wavelength from the top. The resulting fields were probed in polarization direction at a point situated 1 nm away from the surface of the bimetal particles and are shown in Fig. 1b. Comparing the spectra of the bimetal core–shell particles with variable thicknesses of Au shells, the width of the resonance spectrum is changing with d_{Au} and the broadest resonance spectrum is observed for d_{Au}=5 nm. A red shift of ca. 200 nm is observed when changing d_{Au} from 0 nm to 80 nm. Figure 1c shows the maximum field enhancement as a function of the Au shell thickness d_{Au}. When d_{Au} is larger than 10 nm, the maximum field enhancement remains constant. The resonance position and spectral bandwidth are shown in Fig. 1d. For d_{Au} larger than 30 nm, both parameters remain constant and resemble the response of pure Au particles (corresponding to d_{Au}=80 nm). The main reason for this behavior is that when the outer shell is thicker than the skin depth of the material at the excitation wavelength, the inner core does not contribute to the plasmonic response anymore [37].

Enhanced near-field amplitude spectra of the optimized bimetal core–shell NP (with R=80 nm and d_{Au}=5 nm) and of pure Au and Ag NPs (both with R=80 nm) are shown in Fig. 2a. The Ag NP has a sharp resonance at ca. 385 nm with a maximum field enhancement of 3.3 with respect to the excitation field, but the plasmonic absorption is off-resonant to the 800 nm excitation source (also shown in Fig. 2a). The field enhancement for the Au NP is quite low at its maximum at around 600 nm with 2.6. In fact, from 600 nm towards longer wavelength, the field enhancement for Ag and Au is found to be nearly identical. In comparison, the bimetal Ag/Au core–shell nanoparticles exhibit an ultra-broadband plasmonic spectrum peaking at 550 nm with a field enhancement of 3. The spectral bandwidth of the bimetal core–shell particle would facilitate a temporal response of 2.0 fs (obtained from the Fourier transformation of the spectrum).

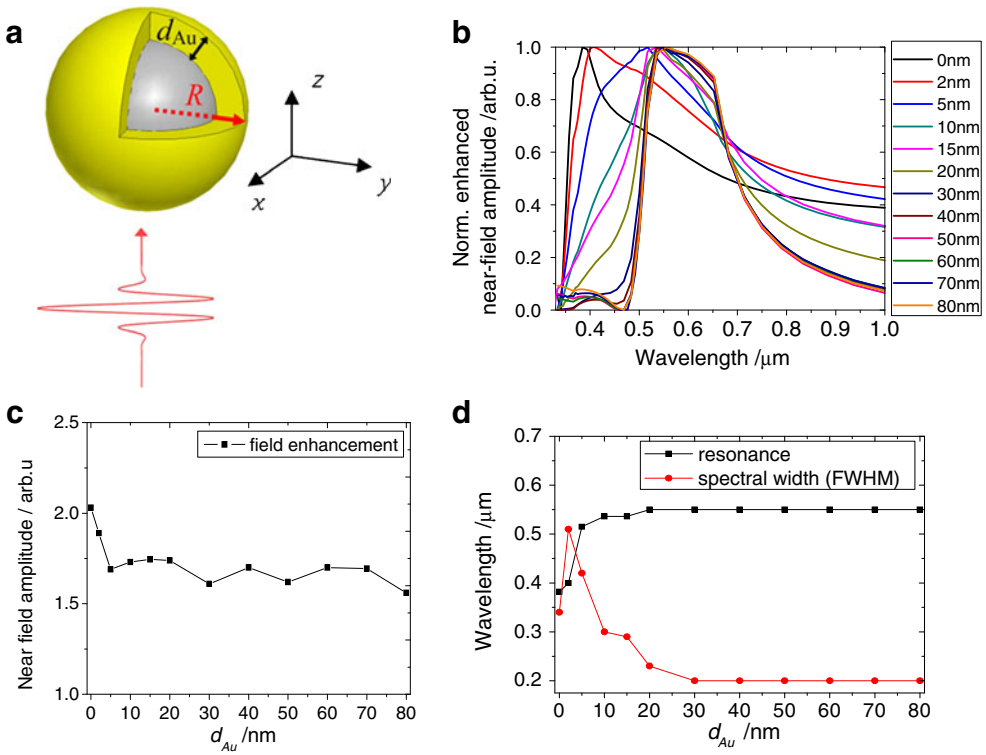

Fig. 1 **a** Ag/Au bimetal sphere with Ag core and Au shell and an overall radius of R. A few-cycle light pulse incident on the nanoparticle is shown schematically below the particle. **b** Normalized enhanced near-field amplitude spectra of bimetal nanoparticles as shown in **a** with variable thicknesses of the Au shell d_{Au}. The overall radius of the nanosphere was kept constant with R=80 nm. **c** Maximum near-field amplitude as a function of the Au shell thickness. **d** FWHM of the plasmonic spectra and resonance position as a function of the Au shell thickness

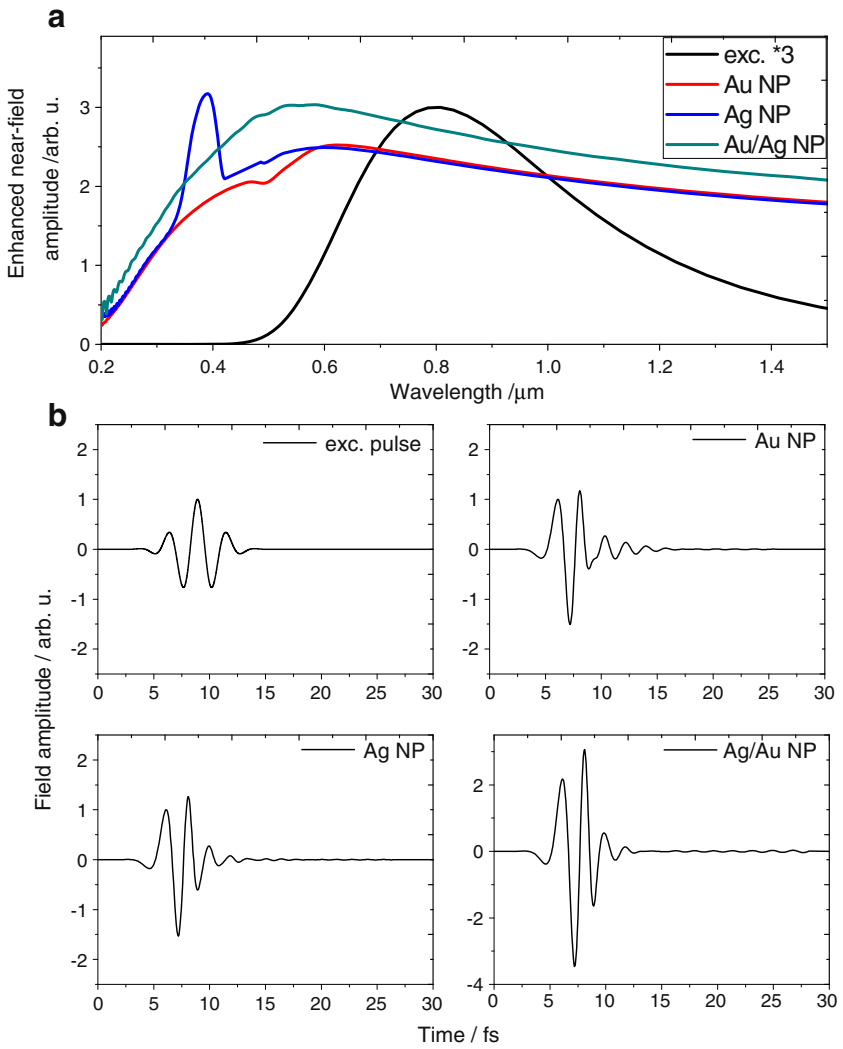

Fig. 2 Enhanced near-field amplitude spectra (**a**) and temporal profiles (**b**) of the excitation field and resulting near-fields of a single Au NP, Ag NP, and Ag/Au core–shell NP with R=80 nm and d_{Au}=5 nm. The excitation pulse is polarized in y-axis direction and its field is normalized to 1 at its maximum

In order to explore the temporal response of these nanostructures, we excited them with an ultrashort, Fourier-limited laser pulse with duration of 4.2 fs full width at half maximum (FWHM) of a Gaussian envelope. The laser pulse has a central wavelength of 800 nm. The results are displayed in Fig. 2b. The fields are probed 1 nm away from the surface of the nanostructures along the polarization direction. For all NPs, the responses are ultrafast (due to the off-resonant excitation) and only vanishing small field oscillations are seen after the excitation field is 0. Remarkably, the field enhancement for the bimetal Ag/Au core–shell particle is the highest among the three studies systems.

Optimization of the Optical Properties of Ag/Au Core–Shell Nanoparticle Dimers

While a single bimetal core–shell nanoparticle allows for an ultra-broadband resonance spectrum, the nanoplasmonic field enhancement of single nanospheres is limited and would not be sufficient, e.g., to be used in high-order harmonic generation [31]. Coupled nanoantennas can exhibit much higher field enhancement [38]. We therefore studied the optical properties of coupled nanosphere dimers, which can be produced by self-assembly methods. By using such methods, the gap between the particles can be controlled very precisely in range of a few nanometers [24, 36], surpassing the spatial resolution of current lithographic techniques.

The gap between adjacent spheres is 2 nm in our calculations. We used identical spheres in the calculations, although chemical synthesis methods will only produce nanospheres with a limited (minimum) width in size distribution [28]. Note, however, that the width of the size distribution of chemically prepared nanoparticles can reach a lower percentage value of the overall radius [28], such that variations in the size of the individual NPs may be neglected for the present studies. The enhanced fields are determined at the center of the gap between the coupled

nanospheres. We investigated the enhanced near-field amplitude spectra of coupled bimetal Ag/Au core–shell nanospheres and compared the results to the responses from coupled pure Au and coupled pure Ag NP antennas. The results are shown in Fig. 3a. The field-enhancement factors in all three cases reach ca. 80. Comparing the three different types of NP dimers, the Ag dimers are found to actually exhibit the broadest spectrum, the center of which is shifted towards the blue with respect to Au dimers. The Ag/Au core–shell dimers exhibit a slightly larger bandwidth than pure Au dimers and the highest field enhancement factors across the spectrum of the excitation pulse. In all three cases, the plasmonic near-field spectrum is spectrally broader than the excitation field. The field distribution around the gap is shown in Fig. 3b for the Ag/Au core–shell dimers.

The temporal profiles of a Fourier transform-limited excitation field with duration of 4.2 fs FWHM and the corresponding near-fields of the various dimers are shown in Fig. 3c. The Au dimer shows a typical response of near-resonant nanoantennas: after reaching a maximum of ca. 80, a smooth nearly exponential decay is observed. For the Ag dimer, the enhanced field reaches a maximum of 120 and decays to nearly 0 after about 10 fs. Interestingly, for the Ag dimer, Fig. 3c shows first oscillations with the laser frequency, which when the excitation pulse vanishes exhibit a higher frequency, corresponding to the eigenfrequency of the dimer (which is blue shifted with respect to the excitation source). A similar behavior, although not as pronounced, can be seen for the Ag/Au core–shell dimer. The latter dimer exhibits the most promising response for applications such as the generation of ultrashort XUV pulses via high-harmonic generation [31]. Here, the field reaches an amplitude of ca. 100 with respect to the excitation field and decays extremely fast to a value below 30 (within ca. 2 cycles). The fast decay of the bimetal NPs is a direct result of the broad bandwidth and furthermore, a result of an excitation that is non-resonant with the peak appearing in the near-field amplitude spectra.

Preparation and Characterization of Small Bimetal Nanoparticles

Since the optical properties of metal nanostructures strongly depend on their size and composition, it is highly desirable to improve the fabrication of novel, ultra-broadband metallic NPs to facilitate their few-cycle laser application.

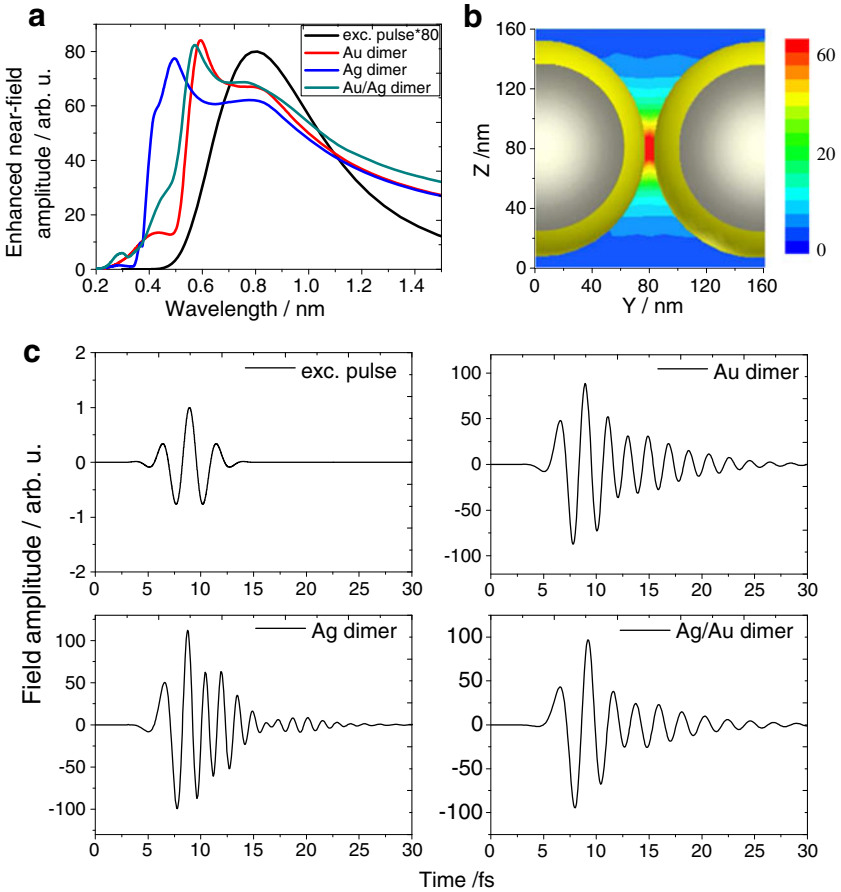

Fig. 3 **a** Enhanced near-field amplitude spectra for Au dimers, Ag dimers, and Ag/Au core–shell dimers with R=80 nm and a gap of 2 nm. For the Ag/Au dimers, the thickness of the outer Au shell d_{Au} is 5 nm. **b** Spatial distribution of maximum near-field amplitudes within the gap of the bimetal nanospheres. **c** Temporal profiles of the normalized Fourier transform-limited excitation field and near-fields of these nanoparticle dimers

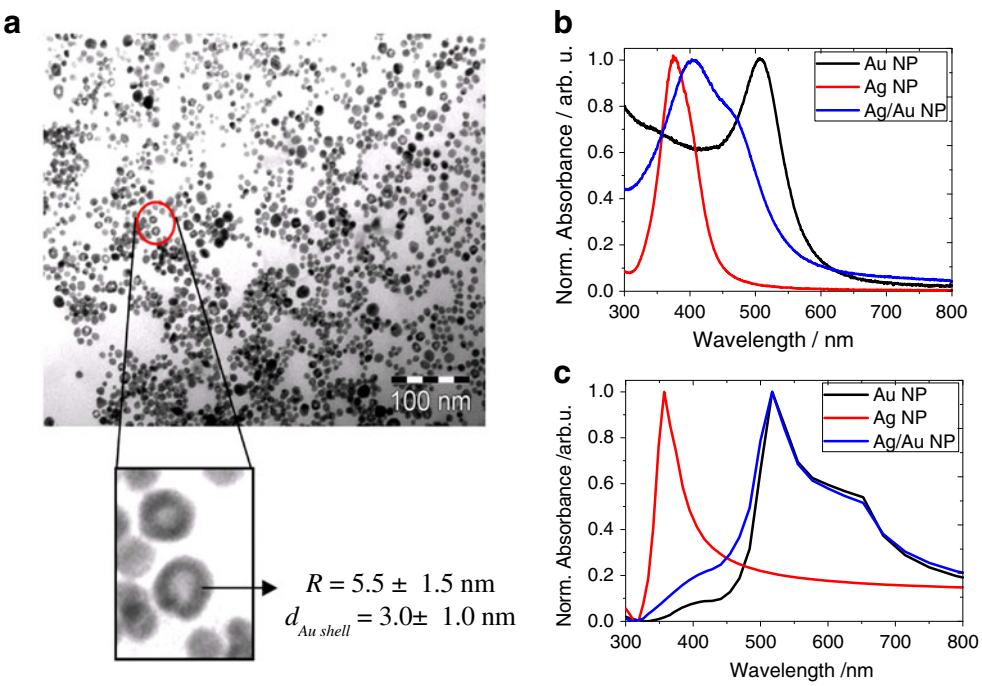

Fig. 4 Characterization of synthesized bimetal NPs: (**a**) TEM image of the bimetal NPs, (**b**) measured plasmon absorption spectra, and (**c**) calculations of Au, Ag, and bimetal NPs with the dimensions given in **a**

The synthesis of metallic and bimetallic nanosystems is usually based on either chemical or physical processes [39]. The most commonly used synthetic method for producing metallic nanoparticles was originally developed by Turkevich et al. [40] and involves the reduction of a metal salt or metal ions by a suitable reducing agent in a liquid. Here, we present our progress towards the fabrication of bimetal NPs, which may ultimately provide much broader bandwidth, supporting both sufficient field enhancement and an ultrafast response for few-cycle applications such as the generation of high-harmonic radiation.

We have synthesized the Au NP from $HAuCl_4 \cdot 3H_2O$. Sodium citrate was applied as reducing agent to stabilize the Au nano-dispersion [41, 42]. The citrate-stabilized Ag NPs were prepared using a silver nitrate solution and sodium borohydride reduction. The concentration of the prepared Au

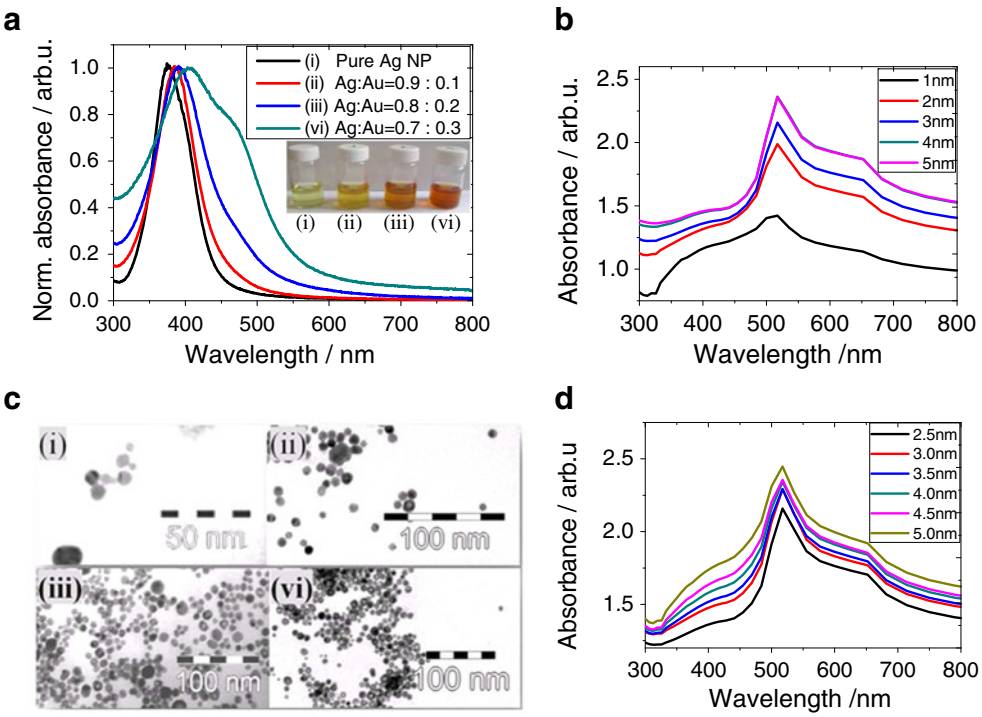

Fig. 5 Plasmon absorption bands (**a**) and TEM images (**b**) of citrate-stabilized pure Ag (*i*) and bimetal Ag/Au NP containing aqueous dispersions with Ag:Au ratios of 0.9:0.1 (*ii*), 0.8:0.2 (*iii*), and 0.7:0.3 (*iv*). When the ratio of Au increases, the spectra exhibit a red shift from 377 to 406 nm and the color of the dispersions turns from yellow to orange. **c**, **d** Calculated absorbance spectra of bimetal NP for the following parameters: (**c**) $R_{\mathrm{Ag\ core}}$ is fixed at 2.5 nm with different thicknesses of outer Au shell d_{Au} from 1 to 5 nm; (**d**) the thickness of outer Au shell d_{Au} is fixed at 3 nm with different $R_{\mathrm{Ag\ core}}$ from 2.5 to 5 nm

and Ag dispersion was 2×10^{-4} M. In the synthesis of the bimetallic Ag/Au core–shell NPs, $HAuCl_4{\cdot}3H_2O$ was dropped into a previously prepared Ag nanoparticle containing dispersion, and sodium citrate was added.

Figure 4a displays a transmission electron microscopy (TEM) image of the bimetallic Ag/Au NPs that were prepared by the synthesis described above. A closed shell is obtained with a 2–3-nm thick Au shell. The dimensions of the synthesized particles are significantly different from our optimized values above due to difficulties in the fabrication of uniform, large diameter Ag spheres. Figure 4b, c shows experimental and theoretical resonant absorption spectra of Au, Ag, and bimetal NPs, respectively. The overall radius R of ca. 5.5 nm of the fabricated NPs shown in Fig. 4a was used in the theoretical calculations. Since the NPs are dispersed in the aqueous solution, the calculations are adjusted to an environment with refraction index $n=1.33$, which results in a minor red shift in comparison to vacuum surrounding the NPs. Figure 4b, c shows similar peak positions in both the experimental and theoretical spectra for pure Au and Ag NPs. The Ag/Au bimetal NPs exhibit a blue shift with respect to the Au NPs in the experiments, which is, however, found to be much larger than in the theory. A possible reason of this deviation is that not all the particles in the experimental dispersion are Ag/Au core–shell NPs, but there is a remainder of pure metal NPs, which affect the spectrum. Although the contributions of pure metal NPs to the absorption spectra cannot be excluded, which makes a quantitative comparison of the experimental spectra of the bimetal particles to theoretical predictions difficult, we may compare NP dispersions with different concentrations of Au and Ag to gain more information from the experimental data.

Figure 5a shows the absorption spectra obtained for various concentrations of Au and Ag in the dispersions and it can be seen that the spectra have a distinct red shift with increasing Au concentration and also exhibit a broader bandwidth. In agreement, a similar shift when varying the Au concentration was also observed in Refs. [43, 44]. Calculations for nanoparticles of the dimensions used in the experiment (determined via TEM imaging, see Fig. 5b) reveal that the core or shell thickness does not influence the absorption spectra strongly (see Fig. 5c, d). The main effect of an increasing Au concentration in the nanoparticle dispersion is therefore likely an increasing amount of Ag/Au core–shell NPs over pure metal NPs.

The characterization of the synthesized bimetal NPs presented here supports their broader spectral bandwidth, which might facilitate their ultrafast response. Unfortunately, despite following the current state-of-the-art in the fabrication of bimetal nanoparticles [45], the synthesis is limited to small NPs. Future work will be directed to the fabrication of larger spheres of bimetal particles (potentially enabled by utilizing an additional dielectric core (e.g., SiO_2/Ag/Au nanoparticles).

Conclusions

Our numerical simulations reveal that optimized bimetal core–shell NPs can provide ultra-broadband plasmonic resonance spectra facilitating an ultrafast temporal response on the order of a few femtoseconds following excitation by a few-cycle field. The latter property is of particular interest and might allow for the production of ultrashort XUV pulses at megahertz repetition rates utilizing nanoplasmonic field enhancement. The efforts in the synthesis of (small) bimetal core–shell Ag/Au NPs, presented in the "Preparation and Characterization of Small Bimetal Nanoparticles" section, support that such particles can exhibit broader spectral bandwidth than pure metal NPs.

Acknowledgments This work was supported by the BMBF under PhoNa, contract number 03IS2101B, the DFG via the Emmy-Noether program and SPP1391. M.F.K. acknowledges support from KAIN within the KSU-MPQ collaboration, and S.L.S. acknowledges a fellowship from the Alexander von Humboldt Foundation.

References

1. Krausz F, Ivanov M (2009) Rev Mod Phys 81:163
2. Corkum PB (1993) Phys Rev Lett 71:1994
3. Maier S, Brongersma M, Kik P, Meltzer S, Requicha A, Koel B, Atwater H (2003) Adv Mater 15:562
4. Stockman MI, Kling MF, Kleineberg U, Krausz F (2007) Nat Photonics 1:539
5. Dombi P, Irvine SE, Rácz P, Lenner M, Kroó N, Farkas G, Mitrofanov A, Baltuška A, Fuji T, Krausz F, Elezzabi AY (2010) Opt Express 18:24206
6. Tuchscherer P, Rewitz C, Voronine DV, García de Abajo FJ, Pfeiffer W, Brixner T (2009) Opt Express 17:14235
7. Kim S et al (2008) Nature 453:757
8. Assefa S, Xia F, Vlasov YA (2010) Nature 464:80
9. Plech A, Kotaidis V, Lorenc M, Boneberg J (2006) Nat Phys 2:44
10. Sun Y, Xia Y (2002) Science 298:2176
11. Wiley B, Sun Y, Mayers B, Xia Y (2005) Chem Eur J 11:454
12. Major K, De C, Obare S (2009) Plasmonics 4:61
13. Sundaramurthy A, Crozier KB, Kino GS, Fromm DP, Schuck PJ, Moerner WE (2005) Phys Rev B (Condens Matter Mater Phys) 72:165409
14. Sundaramurthy A, Schuck PJ, Conley NR, Fromm DP, Kino GS, Moerner WE (2006) Nano Lett 6:355
15. Krenn JR, Schider G, Rechberger W, Lamprecht B, Leitner A, Aussenegg FR (2000) APL 77:3379
16. Mock JJ, Smith DR, Schultz S (2003) Nano Letters 3:485
17. Zhang Z, Weber-Bargioni A, Wu SW, Dhuey S, Cabrini S, Schuck PJ (2009) Nano Lett 9:4505
18. Biagioni P, Polli D, Labardi M, Pucci A, Ruggeri G, Cerullo G, Finazzi M, Duo L (2005) Appl Phys Lett 87:223112

19. Biagioni P, Huang J S, Duò L, Finazzi M, Hecht B (2009) Phys Rev Lett 102:256801
20. Maier SA, Kik PG, Atwater HA (2003) Phys Rev B 67:205402
21. Zijlstra P, Chon JWM, Gu M (2009) Nature 459:410
22. Chah S, Hammond MR, Zare RN (2005) Chem Biol 12:323
23. Ehrhold K, Christiansen S, Gösele U (2008) In plasmonic properties of bimetal nanoshell cylinders and spheres, the Proceedings of the COMSOL Hannover, 2008, Hannover
24. Fan JA, Wu C, Bao K, Bao J, Bardhan R, Halas NJ, Manoharan VN, Nordlander P, Shvets G, Capasso F (2010) Science 328:1135
25. Kelly KL, Coronado E, Zhao LL, Schatz GC (2002) J Phys Chem B 107:668
26. Cortie MB, McDonagh AM (2011) Chem Rev 111:3713
27. Serpell CJ, Cookson J, Ozkaya D, Beer PD (2011) Nat Chem 3:478
28. Xia Y, Xiong Y, Lim B, Skrabalak S (2009) Angew Chem Int Ed 48:60
29. Goulielmakis E et al (2008) Science 320:1614
30. Kling MF, Siedschlag C, Verhoef AJ, Khan JI, Schultze M, Uphues T, Ni Y, Uiberacker M, Drescher M, Krausz F, Vrakking MJJ (2006) Science 312:246
31. Stebbings SL, Süßmann F, Yang Y-Y, Scrinzi A, Durach M, Rusina A, Stockman MI, Kling MF (2011) New J Phys 13
32. Taflove A, Hagness SC (2005) Computational electrodynamics: the finite-difference time-domain method. Artech House Publishers, London
33. Gai H, Wang J, Tian Q (2007) Appl Opt 46:2229
34. Berenger J-P (1994) J Comput Phys 114:185
35. Kottmann JP, Martin OJF (2000) IEEE Trans Antennas Propag 48:1719
36. Li JF, Huang YF, Ding Y, Yang ZL, Li SB, Zhou XS, Fan FR, Zhang W, Zhou ZY, WuDe Y, Ren B, Wang ZL, Tian ZQ (2010) Nature 464:392
37. Homola J (2006) Surface plasmon resonance based sensors. Springer series on chemical sensors and biosensors, vol 4. Springer, Berlin
38. Prodan E, Radloff C, Halas NJ, Nordlander P (2003) Science 302:419
39. Zhang J, Noguez C (2008) Plasmonics 3:127
40. Turkevich J, Stevenson PC, Hillier J (1951) Discuss Faraday Soc 11:55
41. Majzik A, Patakfalvi R, Hornok V, Dékány I (2009) Gold Bull 42:113
42. Majzik A, Fülöp L, Csapó E, Bogár F, Martinek T, Penke B, Bíró G, Dékány I (2010) Colloid Surf B Biointerfaces 81:235
43. Link S, Wang ZL, El-Sayed MA (1999) J Phys Chem B 103:3529
44. Belotelov VI, Carotenuto G, Nicolais L, Longo A, Pepe GP, Perlo P, Zvezdin AK (2006) J Appl Phys 99:044304
45. Halas N, Lal S, Chang W-S, Link S, Nordlander P (2011) Chem Rev 111:3913